Int J Adv Manuf Technol (2006) 27: 911–917
DOI 10.1007/s00170-004-2273-6

ORIGINAL ARTICLE

**K.M. Rezaur Rahman · M. Rahman · K.S. Neo · M. Sawa · Y. Maeda**

# Microgrooving on electroless nickel plated materials using a single crystal diamond tool

Received: 10 February 2004 / Accepted: 28 May 2004 / Published online: 23 February 2005


**Abstract** Diamond tools are used in ultra precision machining for their outstanding hardness and crystalline structure, which enable the fabrication of very sharp cutting edges. Single crystal diamond tools are thus extremely useful to machine electroless nickel-plated dies which are generally used for making molds for optical components. This paper deals with the objective to evaluate the performance and suitability of a single crystal diamond tool during microgrooving on electroless nickel plated workpieces. Effects of different machining parameters on overall machining performance were also investigated. The experimental results revealed that long distance (50 km) machining of microgrooves on electroless nickel is possible with a single crystal diamond tool without any significant tool wear. Some groove wear on the rake face were found after machining 28.5 km. No evidence of chipping or wear had been observed on the flank face during the total machining length. The surface roughness range of the machined workpieces was found to be 4–6 nm. Both thrust and cutting components of the machining forces showed an increasing trend with increasing machining distance, though magnitude of the thrust forces were found to increase more than the cutting forces.

**Keywords** Electroless nickel · Microgroove · Single crystal diamond tool · Surface roughness · Tool wear

## 1 Introduction

The ultra-precision machining at present is a key technique for the manufacturing of components used for the systems in a variety of advanced science and technology applications. Through the 1970s, the technique was applied for the production of a variety of optical components for its high precision, versatility and lower overall manufacturing cost. More recent applications of ultra-precision machining are for the manufacturing of optical parts with sophisticated form and extremely high geometrical and surface quality [1]. The development of ultra-precision machining technology relies on the technology of tools, such as single-crystal diamond tools and machine elements including air bearings, air slides, granite beds mounted by air, and precise position-control technology. The primary goal of ultra-precision machining is to achieve an optical surface of a few nanometer RMS by using a single crystal diamond tool [2]. Single-crystal diamond machining offers a very time-and-cost effective method for producing both large-diameter metal optics and metal optics with highly aspheric contours; however, the process has a serious limitation in that only soft, FCC metals have been found to be readily machinable with single-point diamonds. The most popular metals for diamond machining, namely copper and aluminum, offer surfaces that can easily be ruined by abrasion and corrosion from cleaning and handling [3]. It is important to note, however, that not all materials are machinable by diamond tools. For example, materials that generally react with carbon are not considered diamond turnable. A very useful alternative to the soft metals is a nickel-phosphorous alloy chemically deposited from an aqueous solution. This material is commonly known as "electroless nickel". Electroless nickel is hard, very corrosion resistant, and best of all, diamond machines beautifully [4].

Studies have been conducted by researchers [4–6] on face turning of electroless nickel and to determine the wear characteristics of diamond tools considering different crystal orientations and infrared absorption quality for short cutting distance. However, long distance machining of microgrooves on electroless nickel and related machining phenomenon are not well investigated.

This paper attempts to evaluate the performance of a single crystal diamond tool during long distance machining of microgrooves on electroless nickel plated materials. The effects of spindle speed, infeed rate and dwell time on machining per-

K.M. Rezaur Rahman · M. Rahman (✉) · K.S. Neo
Department of Mechanical Engineering,
National University of Singapore,
9 Engineering Drive 1, Singapore 117576
E-mail: mpemusta@nus.edu.sg
Tel.: +65-68742168
Fax: +65-67791459

M. Sawa · Y. Maeda
Production Engineering Research Laboratory,
Hitachi Ltd., Kanagawa, Japan

formance were also observed. The machining performance was evaluated in terms of tool wear, cutting forces and roughness of the machined surfaces.

## 2 Experiments

The experiments were carried out on a TOSHIBA ULG-100 ultraprecision machine with a capability of 10 nm positioning resolution. A single crystal artificial diamond tool with 0° rake and 7° clearance angle with a crystal orientation of {110} was used to machine the microgrooves on electroless nickel plated workpieces. The experimental setup and machining conditions are shown in Fig. 1 and Table 1, respectively. The cutting tool was preformed with a plane angle of 90°15' to generate the microgrooves. Schematic sketches of the cutting tool are shown in Fig. 2. Electroless nickel plated workpieces with a phosphorous content of 10 to 12% (w/w) were used in their as-deposited condition. Each workpiece was 100 mm in diameter with a plating thickness of 100 μm and a central recess of 5 mm diameter. During the experiments the tool traveled from the periphery to the center of the workpiece. The machining of microgrooves of 4.5 μm depths was done by the plunge cut method. The cross section of the grooves on the machined workpiece is shown schematically in Fig. 3. Kerosene based oil mist was used during the experiments to achieve a better surface finish and vacuum suction was used to facilitate chip removal from the tool workpiece interface.

The tool and workpiece surfaces were checked with optical microscopy after each five passes. The cutting and thrust forces were measured for every pass. The cutting component ($F_c$) acts in the direction normal to the cutting tool face and the thrust component ($F_t$) normal to the workpiece surface as shown in Fig. 1. Surface roughnesses of the machined workpieces were also determined after every pass during the experiments. Replication tests of the tool cutting edge and plunge tests were carried out on oxygen free high conductivity (OFHC) copper pieces after each 10 km of machining distance to observe the change in the cutting tool edge profile. The method of Li et al. [7] was used to determine the change in edge radius of the tool.

The different machining parameters considered to observe their effects on the machining performance are tabulated in Table 2. Starting with 100 rpm spindle speed, 0.1 μm/rev infeed rate and 0.01 sec as the dwell time, spindle speed was varied in the next four experiments keeping the other two parameters constant. During the sixth to ninth experiment, fixing the spindle speed and dwell time at 1000 rpm and 0.01 sec respectively, the infeed rate was varied. In a similar manner, from the 10th to 13th

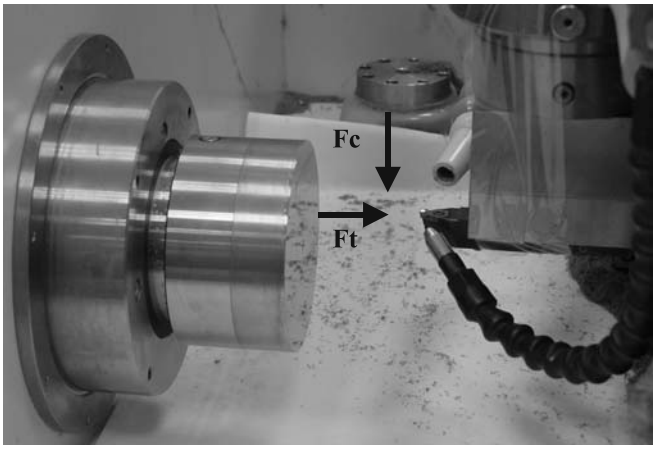


**Fig. 1.** Experimental setup

**Table 1.** Experimental conditions

| | |
|---|---|
| Depth of cut (μm) | 4.5 |
| Spindle speed (rpm) | 1000 |
| Infeed rate (μm/rev) | 0.5 |
| Dwell time (sec) | 0.1 |

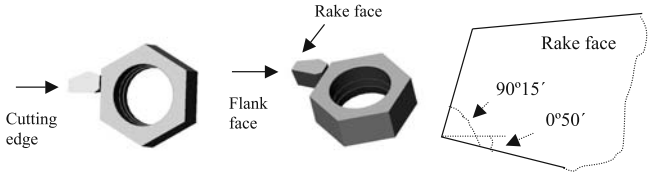


**Fig. 2.** Different views and geometry of the cutting tool

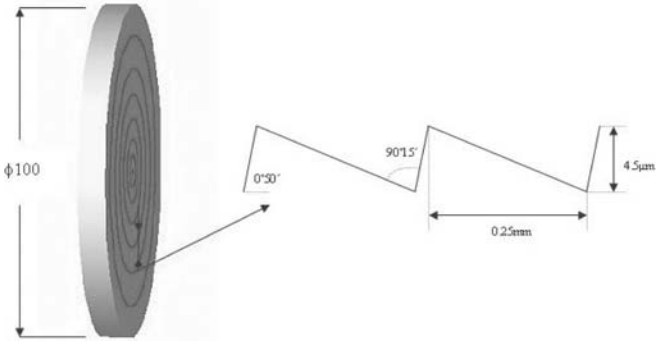


**Fig. 3.** Schematic details of the groove cross section

**Table 2.** Combination of different machining parameters to observe the effects on cutting performance

| Experiment No. | Spindle speed (rpm) | Infeed rate (μm/rev) | Dwell time (sec) |
|---|---|---|---|
| 1 | 100 | 0.1 | 0.01 |
| 2 | 250 | 0.1 | 0.01 |
| 3 | 500 | 0.1 | 0.01 |
| 4 | 750 | 0.1 | 0.01 |
| 5 | 1000 | 0.1 | 0.01 |
| 6 | 1000 | 0.5 | 0.01 |
| 7 | 1000 | 1 | 0.01 |
| 8 | 1000 | 2 | 0.01 |
| 9 | 1000 | 3 | 0.01 |
| 10 | 1000 | 3 | 0.05 |
| 11 | 1000 | 3 | 0.1 |
| 12 | 1000 | 3 | 0.2 |
| 13 | 1000 | 3 | 0.5 |

experiments, dwell time was varied keeping the spindle speed and infeed rate constant at 1000 rpm and 3 μm/rev.

The measurements and equipments used during the experiments are listed below:

1. Replication (grooves of 2 μm depth) and plunge tests (indentations of 2 μm depth) on OFHC copper disks to detect change in the tool edge profile and measure cutting edge radius using atomic force microscopy and scanning electron microscopy.
2. Optical and electron microscopy observation of the tool and machined workpieces using a Nomarski optical microscope (Olympus STM-6) and scanning electron microscope (SEM) (JSM-5500).
3. Surface roughness (both $R_a$ and $R_y$) of the machined workpieces using a Mitutoyo formtracer CS 5000.
4. Both cutting and thrust components of machining forces using Kistler piezoelectric 3 component dynamometer in conjunction with a Kistler 3 channel charge amplifier and a recorder for data recording.
5. Hardness (Vickers scale) of the workpieces using a Mitutoyo AVK C2 hardness tester.

## 3 Results and discussion

### 3.1 Wear behavior of cutting tool

The experiments were carried out for 50 km of cutting distance with the conditions stated in Table 1. The same single crystal diamond cutting tool was used for the total machining distance. No significant tool wear was observed before 28.545 km of the machining distance. Several grooves were observed on the rake face of the cutting tool. There was no regular shape of the grooves to identify them as the cause of a certain machining condition. The number of grooves increased with increasing cutting distance up to 50.145 km. The gradual increment of grooves on the rake face can be observed in Fig. 4.

The maximum length of a groove measured from the cutting edge was 0.0265 mm. The grooves were seen up to 0.25 mm on the rake face from the tip of the cutting edge. The pitch of the machined microgrooves was 0.25 mm, which indicates that the groove wear zone spread over the whole pitch length.

The SEM micrograph of the tool rake face is shown in Fig. 5 at 1500 times magnification after reaching 50.145 km of the cutting distance. The photograph shows that the grooves started to propagate after a certain distance from the cutting edge. For this reason, the surface roughness of the machined workpieces were noticed to be unaffected by the groove wear. The values of the surface roughness were carefully observed after the first initiation of the grooves after 28.545 km of the machining distance.

The flow of chips along the tool rake face might cause the grooves to appear. Electroless nickel is very hard and the maximum hardness observed for the workpieces was 566 Hv. The pressure on the rake face of the tool was quite high and the chips or grains of electroless nickel acted as abrasive powder flowing over the rake face thus creating the grooves. A vacuum suction system was used to remove the chips from the tool-workpiece interface, which might cause the irregular shape of the grooves. Oomen et al. [8], observed the same pattern of grooves while face turning electroless nickel specimens for 50 km of cutting distance.

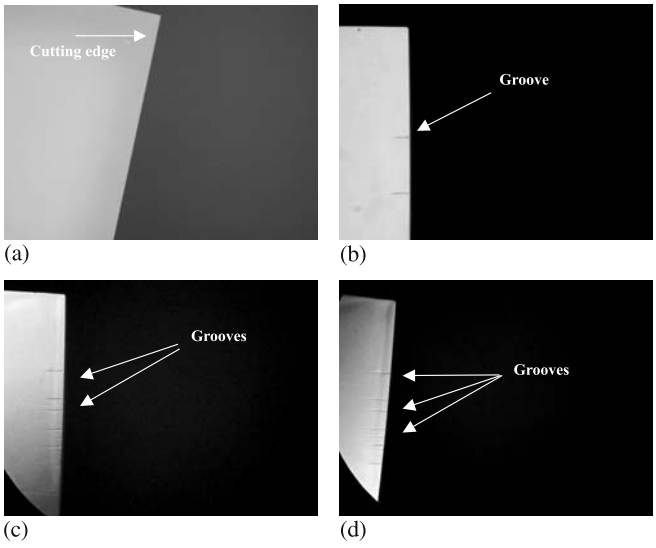


**Fig. 4a–d.** Nomarski photographs of tool rake face after **a** 21.255, **b** 28.545, **c** 41.235 and **d** 50.145km of cutting distance (magnification: ×500)

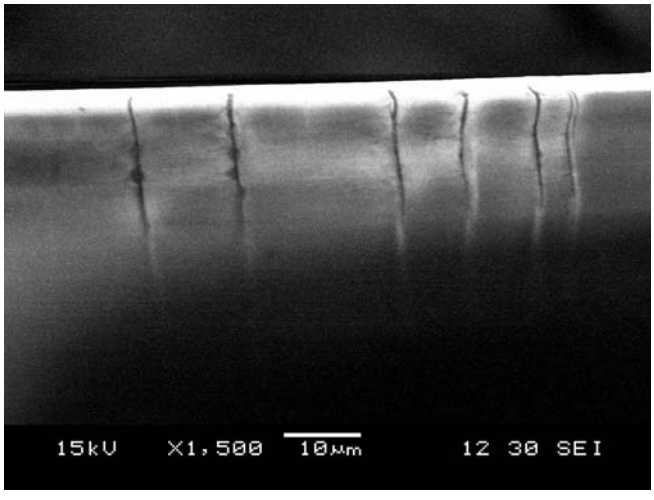


**Fig. 5.** SEM micrograph of tool rake face after 50.145 km cutting distance

The flank face of the cutting tool was observed in the same manner as the rake face. There was no sign of flank wear during the total length of the cutting distance. No chipping was observed on the flank face of the tool. The photographs of the tool flank face are shown in Fig. 6 at different cutting distances. It can be observed from the photographs that there was a rounding off effect on the cutting edge. The sharpness of the tool cutting edge was changed with increasing cutting distance. The replication tests of the tool cutting edge on copper pieces supported this rounding off phenomenon, although the surface roughnesses of the machined workpieces were still unaffected. The primary

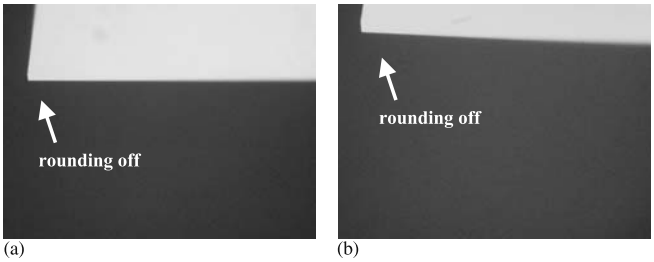


(a) (b)

**Fig. 6a,b.** Nomarski photographs of tool flank face after **a** 21.255 and **b** 50.145 km cutting distance (magnification: ×500)

profiles (P-profile) of the roughness of the replication tests on copper pieces showed an increase in surface roughness, which is in agreement with the optical view of the cutting edge rounding off of the tool. As the experiments were carried out using the plunge cut method, the tool tip had the most significant role to play in machining microgrooves on the workpieces. This might have resulted in gradual rounding off of the tool tip.

### 3.2 Observed surface roughness with cutting distance

The surface roughnesses of the machined workpieces were checked after each pass to observe any change in the surface caused from tool wear. Three different sections from the workpieces were selected for checking the surface roughness. A section near the periphery, one section near the center and another in between the former two sections were considered. The measurements were taken in the radial direction of the workpieces. Each measuring length consisted of 5 mm of each section. The final roughness value was selected taking the average of those three sections. No significant change in surface roughness was actually observed during the experiments. The variation of the surface roughness with the cutting distance is graphically represented in Fig. 7. It can be observed that the roughness of the machined surfaces remained almost constant from the beginning of the experiments. This is due to very insignificant tool wear during the machining process. The lowest roughness value achieved during machining was 4 nm. At the end of the experiments, the observed surface roughness was 5 nm. A sample photograph of the machined workpiece is shown in Fig. 8.

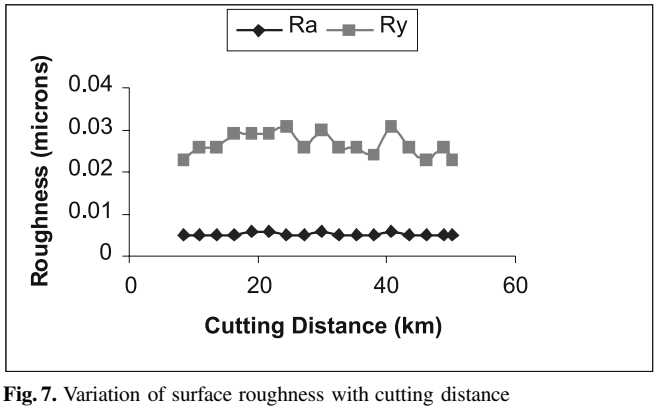


**Fig. 7.** Variation of surface roughness with cutting distance

**Fig. 8.** Sample photograph of the machined workpiece (magnification: ×100)

### 3.3 Machining forces with cutting distance

The variations of the two components of forces during the experiments are represented graphically in Fig. 9. It can be observed that both the cutting and thrust forces increased with increasing cutting distance. From the beginning of the experiments the thrust forces were observed to have a higher magnitude than the cutting forces.

The increase in the cutting force during the total experimental length was not very significant. On the other hand, for the thrust forces the increment was a bit high. This phenomenon may be explained by the change in the cutting edge radius of the tool. It is observed that the cutting edge radius was increased with increasing cutting distance. Initially, the cutting edge radius of the tool was measured as about 22 nm, which became about 43 nm after reaching 50 km of the cutting distance. This increase in cutting edge radius might cause the thrust forces to increase significantly with the cutting distance [9]. Optical observation of the tool did not reveal any significant wear to affect the forces.

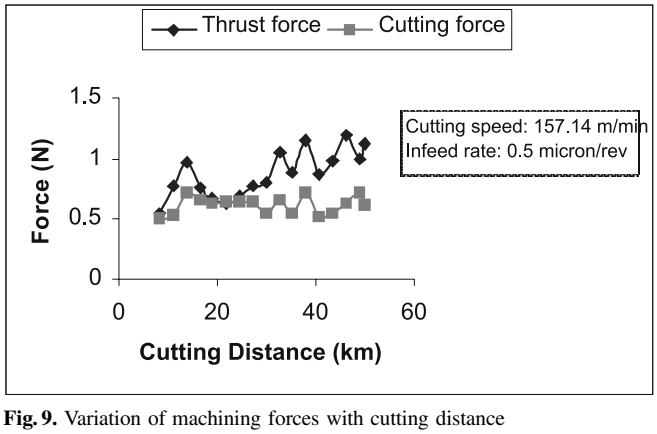


**Fig. 9.** Variation of machining forces with cutting distance

### 3.4 Effect of spindle speed on surface roughness

In ultraprecision machining, the arithmetic surface roughness generally decreases with increasing spindle speed. It has been observed that the width of the shear zone decreases with increasing spindle speed, which might lead to a better machined surface at a higher spindle speed. Obviously, there is an optimum spindle speed for different machining operations at different conditions, by which the arithmetic roughness can be minimized [10, 11]. The variation of surface roughness observed during the experiments with spindle speed is shown in Fig. 10. It has been observed from the figure that surface roughness was similar for different spindle speeds except at 500 rpm. It is not possible to draw any conclusion regarding the effect of spindle speed on surface roughness using this range of spindle speeds. Further studies should be carried out to realize this behavior.

### 3.5 Effect of infeed rate and dwell time on surface roughness

The effect of infeed rate on the surface roughness observed during the experiments is shown in Fig. 11. It has been observed that the change in infeed rate from 0.1 to 3 μm/rev does not affect the surface roughness at all. As the depth of cut of each microgroove was 4.5 μm, it can be expected that there would not be much variation in the surface roughness due to the effect of the infeed rate range used.

The primary application for the dwell command is to allow time for the tool pressure to be relieved. When grooving on a turning center it is preferable to include a short pause after the grooving tool has reached the groove bottom to allow the grooving tool to clean up the bottom of the groove.

The experimental results on the variation of surface roughness with dwell time are represented in Fig. 12. Ideally, surface roughness should decrease with increasing dwell time. However, during this study, it has been observed that the surface roughness decreases with increasing dwell time up to a certain limit and then increases. So there might be a critical value of dwell time depending on machining conditions.

### 3.6 Variation of machining forces with cutting parameters

The effects of spindle speed and infeed rate on cutting forces are shown in Figs. 13 and 14, respectively. It can be observed from the figures that both the cutting and thrust forces increased with increasing spindle speed and infeed rate. With the increase

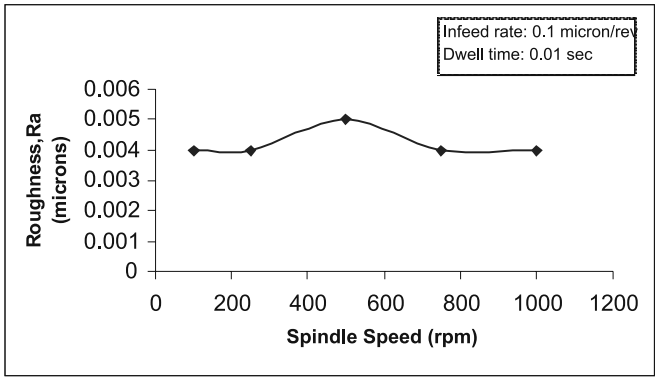


**Fig. 10.** Effect of spindle speed on surface roughness

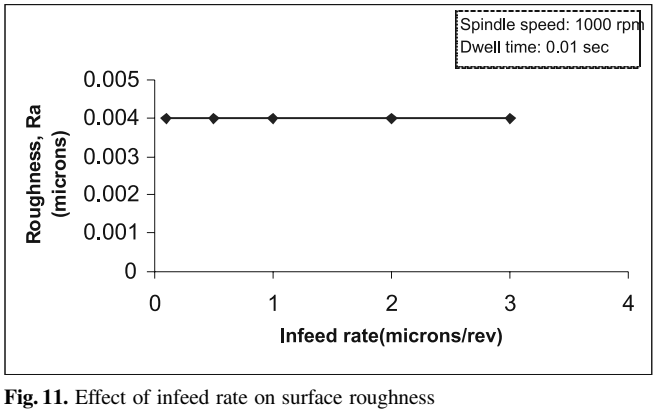


**Fig. 11.** Effect of infeed rate on surface roughness

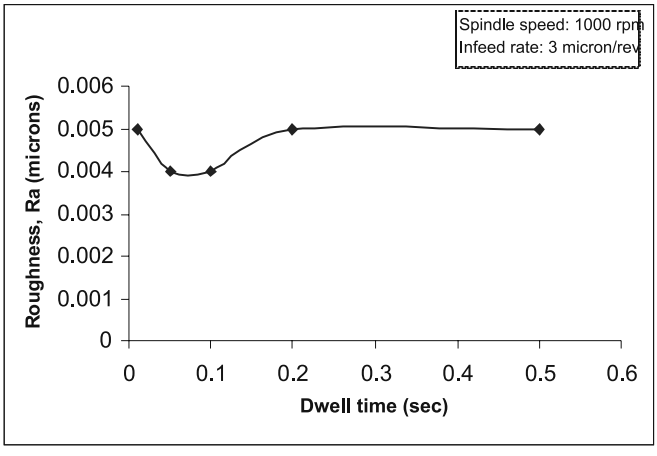


**Fig. 12.** Effect of dwell time on surface roughness

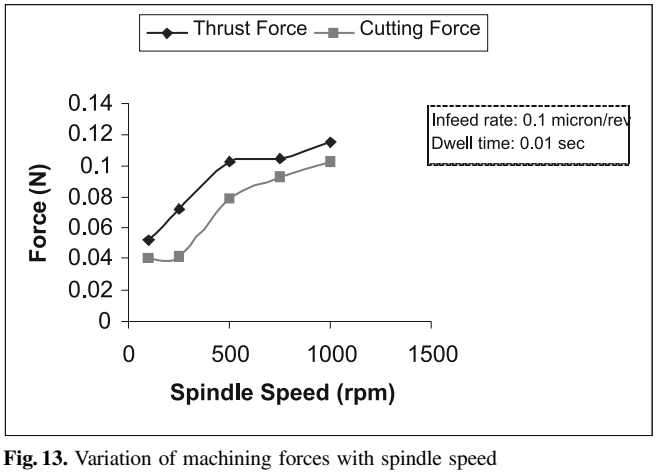


**Fig. 13.** Variation of machining forces with spindle speed

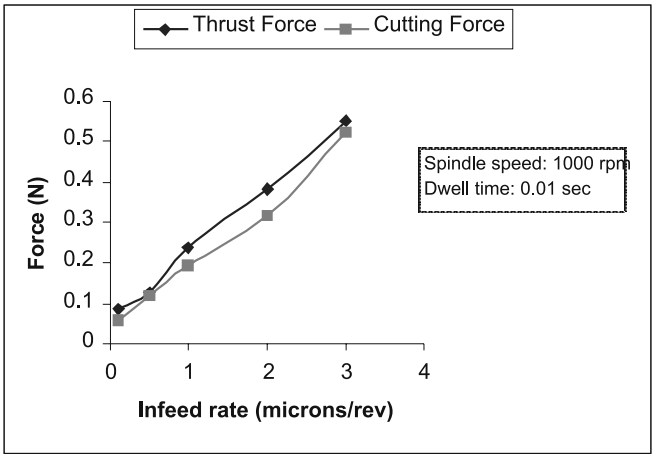


**Fig. 14.** Variation of machining forces with infeed rate

of infeed rate, the interaction between the tool face and workpiece and the stress on the cutting tool increases which might be the cause of an increment in the forces. In the case of spindle speed, with increasing spindle speed both the cutting speed and material removal rate increases which might be a cause of the increment in forces [9]. Researchers observed that with increasing cutting speed there is an increase in the acceleration of the chip removed, which might causes the increment of the forces [12]. Another explanation of this phenomenon is that with increasing cutting speed, there is an increased strain rate on the workpiece material causing an increase in the yield strength of the material through strain hardening. This increment in the yield strength of the material may cause an increment in the thrust and cutting forces [12, 13].

### 3.7 Effect of phosphorous content on hardness of electroless nickel

The material removal process is not governed solely by the cutting tool but also critically by the work material. Work materials must be chosen which give an acceptable machinability on which the nanometric surface finish can be achieved [1]. For electroless nickel, phosphorous content has a great influence on both hardness and structure. It was also observed that the diamond machines a workpiece well with a higher phosphorous content [14]. Randomly chosen workpieces were tested for the phosphorous content and hardness. It was observed that the hardness of the workpieces decrease with increasing phosphorous content. The results of the hardness tests is shown graphically in Fig. 15, which is in agreement with the results found by Syn et al. [14] and Pramanik et al. [9].

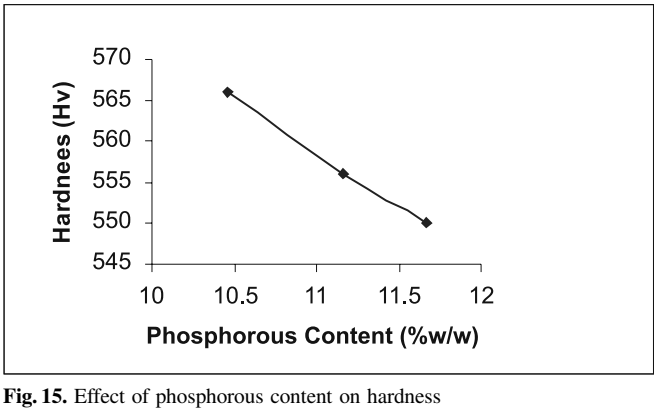


**Fig. 15.** Effect of phosphorous content on hardness

## 4 Conclusions

This study has been carried out to investigate the suitability of a single crystal diamond tool for machining of microgrooves for a long distance. The effects of different machining parameters were also observed. The following conclusions can be drawn from this study:

- The single point diamond tool used in this study showed the suitability of its use to machine microgrooves on electroless nickel for a long distance (50 km) without any significant tool wear.
- The minimum surface roughness achieved during this study was 4 nm and not much variation of surface roughness was observed during the total machining distance.
- Some groove wear on the rake face were observed. The number of these wear increased with increasing machining distance. However, there was no evidence of deterioration of the machined surface quality due to these wear.
- Both cutting and thrust components of the machining forces showed an increasing trend with machining distance. The thrust forces increased more than the cutting forces due to the increment in the cutting edge radius with the machining distance.
- It was observed that with the increase of spindle speed and infeed rate both the thrust and cutting components of machining forces increase.

## References

1. Ikawa N, Donaldson RR, Kumanduri R, Konig W, Mckeown PA, Moriwaki T, Stowers IF (1991) Ultra-precision metal cutting - the past, the present and the future. Ann CIRP 40(2):587–593
2. Weule H, Hüntrup V, Tritschler H (2001) Micro-cutting of steel to meet new requirements in miniaturization. Annals CIRP 50(1):61–65
3. Childress FG, Eary SH, McLaughlin JE (1978) Cleaning and protecting LASL laser mirrors. Y/DA-7591, Union Carbide Corporation-Nuclear Division, Oak Ridge Y-12 Plant, Oak Ridge, TN
4. Casstevens JM, Daugherty CE (1978) Diamond turning optical surfaces on electroless nickel. Precis Mach Optics SPIE 159:109–113
5. Syn CK, Taylor JS, Donaldson RR (1986) Diamond tool wear vs. cutting distance on electrolesss nickel-mirrors. Proc SPIE on Ultra-Precision Machining and Automated Fabrication of Optics 676:128–140
6. Wada R, Kodama H, Nakamura K (1980) Wear characteristics of single crystal diamond tool. Ann CIRP 29(1):47–52
7. Li XP, Rahman M, Liu K, Neo KS, Chan CC (2003) Nano-precision measurement of diamond tool edge radius for wafer fabrication. J Mater Process Technol 140:358–362

8. Oomen JM, Eisses J (1992) Wear of monocrystalline diamond tools during ultra-precision machining of non ferrous metals. Precis Eng 14(4):206–218
9. Pramanik A, Neo KS, Rahman M, Li XP, Sawa M, Maeda Y (2003) Cutting performance of diamond tools during ultra-precision turning of electroless-nickel plated die materials. J Mater Process Technol 140(1-3):308–313
10. Cheung CF, Lee WB (2001) Characterisation of nanosurface generation in single-point diamond turning. J Mach Tools Manuf 41: 851–875
11. Bhattacharya A (1996) Metal cutting theory and practice. New Central Book Agency, Calcutta, India
12. Jared BH, Dow TA (2000) Investigation and prediction of chip geometry in diamond turning. Precis Eng 24:88–96
13. Trent EM, Wright PK (2000) Metal cutting, 4th ed. Butterworth-Heinemann, MA, USA
14. Syn CK, Dini JW, Taylor JS, Mara GL, Vandervoort RR, Donaldson RR (1985) Influence of phosphorous content and heat treatment on the machinability of electroless nickel deposits. Proc Electroless Nickel Conference IV, Chicago, IL, 1-5 May 1985